PHYSICAL REVIEW A **69**, 042318 (2004)

Components for optical qubits encoded in sideband modes

E. H. Huntington*
Centre for Quantum Computer Technology, School of Information Technology and Electrical Engineering, University College, The University of New South Wales, Canberra ACT 2600, Australia

T. C. Ralph
Centre for Quantum Computer Technology, Department of Physics, The University of Queensland, St Lucia QLD 4072, Australia
(Received 3 November 2003; published 22 April 2004)

We describe a scheme for the encoding and manipulation of single photon qubits in optical sideband modes using standard optical elements. We propose and analyze the radio frequency half-wave plate, which may be used to make arbitrary rotations of a state in the frequency basis, and the frequency beamsplitter, which may be used to separate (or combine) photons of different frequencies into (from) different spatial modes.

DOI: 10.1103/PhysRevA.69.042318 PACS number(s): 03.67.−a, 42.50.−p

I. INTRODUCTION

Quantum information can be encoded and manipulated using single photon states. Many in-principle demonstrations of quantum information tasks have now been accomplished in single photon optics including quantum cryptography [1], quantum dense coding [2], and quantum teleportation [3]. More recently, two qubit gates have been realized [4,5] using conditional techniques [6]. Such experiments typically make use of polarization to encode the qubits. However, polarization is not the only photonic degree of freedom available to the experimentalist. For example, schemes in which the timing [7] or occupation [8] of optical modes are the quantum variables have also been realized.

We consider here another possibility: a scheme whereby an optical qubit is encoded in the occupation by a single photon of one of two different frequency modes. Two optical frequency basis states, separated by radio or microwave frequencies, would be sufficiently close together that they could be manipulated with standard electro-optical devices but still be clearly resolvable using narrowband optical and optoelectronic systems. There is also the tantalizing possibility of implementing such a scheme using commercial optical fiber technologies. Hence, such an encoding scheme is attractive from the perspective of developing stable, robust, and ultimately commercially viable optical quantum information systems.

The experimental attraction of developing optical fiber-based quantum optical systems is clear. For example, there is an ongoing interest in developing nonclassical optical sources that will be well suited to optical fibers and optical fiber technologies [9–11]. Indeed a quantum key distribution (QKD) scheme using radio frequency amplitude and phase modulation as the conjugate bases has recently been demonstrated using optical fibers and fiber technologies [12].

If general experiments in the "radio frequency basis" (rf basis) are to become viable, we would require analogies of the tools of the trade used in polarization encoding schemes. These tools are principally the half-wave plate (HWP), which is used to make arbitrary rotations of a state in the polarization basis, the polarizing beamsplitter (PBS), which is used to separate (or combine) photons into (from) different spatial and polarization modes, and the quarter-wave plate (QWP), which is used to introduce relative phase shifts between the two bases.

The principle contribution of this work is to introduce and then analyze a device which produces arbitrary rotations in the rf basis, a "radio frequency half-wave plate" (rf-HWP). A necessary component of the rf-HWP is a "frequency beamsplitter" (FBS), the rf-basis analogue of the PBS. Previous papers have described a device based on a Fabry-Perot cavity which could be used as a FBS [13,14]. Here, we shall outline a technique that is far less experimentally challenging than that discussed in Ref. [13]. We note that relative phase shifts (that is, QWP action) can be achieved through propagation.

II. IN PRINCIPLE

In order to illustrate the physics of the device, let us first take an idealized example of an encoding scheme which makes use of the radio frequency basis. Consider the logical basis whereby

$$|0\rangle_L = |1\rangle_{-\Omega}|0\rangle_{+\Omega},$$

$$|1\rangle_L = |0\rangle_{-\Omega}|1\rangle_{+\Omega}, \tag{1}$$

where $|0\rangle_L$ and $|1\rangle_L$ denote the logical states of the qubit, and the notation $|n\rangle_{\pm\Omega}$ denotes an n photon state at the frequency $\pm\Omega$ relative to the average or carrier frequency ω_0. We shall assume that the states are indistinguishable apart from their frequencies, and we note that Ω is taken to be a radio or microwave frequency in the range of tens of megahertz to a few gigahertz. It is convenient to write the states of Eq. (1) in the form

*Email address: e.huntington@adfa.edu.au

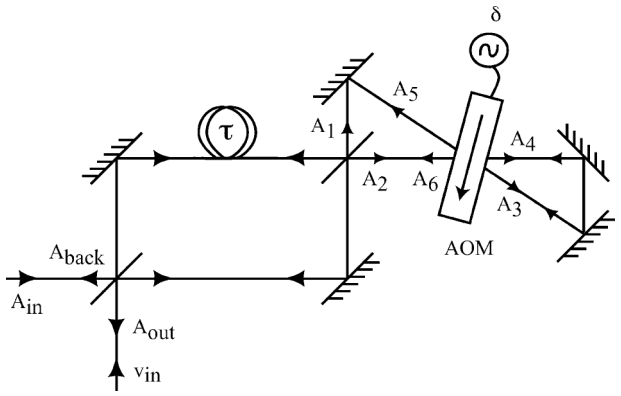

FIG. 1. A schematic diagram of the proposed system. All of the beamsplitters are 50% transmitting, the internal fields are labeled as A_k, and the arrows indicate directions of propagation of optical fields. The differential time delay in the two arms of the Mach-Zehnder interferometer is indicated by the time delay τ. The abbreviation AOM stands for acousto-optic modulator and the arrow in the AOM indicates the direction of propagation of the acoustic wave in the device. The frequency of the rf source used to drive the AOM is δ.

$$|0\rangle_L = A(-\Omega)^\dagger|0\rangle,$$
$$|1\rangle_L = A(+\Omega)^\dagger|0\rangle, \tag{2}$$

where $A(\omega)^\dagger$ is the creation operator for the ω frequency mode. As all the elements in our device are passive (energy conserving), we can obtain the state evolution produced through the device by considering the Heisenberg evolution of the relevant operators.

Figure 1 schematically illustrates the rf-HWP. We shall assume that all of the beamsplitters are 50% transmitting in our analysis of the system depicted in Fig. 1. We shall additionally make use of the symmetric beamsplitter convention [15]. Let us denote the "forward traveling" beams as those propagating to the right-hand side of Fig. 1, and the "backward traveling" beams as those propagating to the left-hand side.

In the Heisenberg picture, we define the annihilation operator for the input mode at a particular Fourier frequency ω relative to the carrier as $A_{in}(\omega)$. We also define an ancilla field $\hat{v}_{in}(t)$, initially in a vacuum state, entering the device vertically from the bottom. Figure 1 defines a number of internal annihilation operators for the rf-HWP, as well as two output fields. The output of interest is A_{out}.

If we take the logical basis as defined in Eqs. (1) and (2), we become specifically interested in the operators, $A_k(\Omega)$ and $A_k(-\Omega)$, where $k=in, 1\cdots 6$, *out*, and *back*. We shall make use of the relation that $A_k^\dagger(\omega)=A_k(-\omega)^\dagger$ [16] to find the relevant creation operators.

The first stage of the rf-HWP is essentially a highly asymmetric Mach-Zehnder interferometer. The annihilation operators for the forward traveling outputs of the Mach-Zehnder interferometer at the frequency ω may be written as

$$A_1(\omega) = \tfrac{1}{2}[A_{in}(\omega)(-e^{i\phi}e^{i\omega\tau}+1) + iv_{in}(\omega)(e^{i\phi}e^{i\omega\tau}+1)],$$
$$A_2(\omega) = \tfrac{1}{2}[iA_{in}(\omega)(e^{i\phi}e^{i\omega\tau}+1) + v_{in}(\omega)(e^{i\phi}e^{i\omega\tau}-1)], \tag{3}$$

where A_1 and A_2 are defined in Fig. 1, τ is the differential time delay introduced into one of the arms of the interferometer, and $\phi=\omega_0\tau$ is the phase shift acquired by a field at the carrier frequency.

Choosing the time delay τ in the interferometer such that $\phi=\pi/2$ and $\Omega\tau=\pi/2$, the creation operators for the forward traveling outputs of the Mach-Zehnder interferometer at the frequencies $\omega=\pm\Omega$ are

$$A_1(\Omega)^\dagger = A_{in}(\Omega)^\dagger, \quad A_1(-\Omega)^\dagger = -iv_{in}(-\Omega)^\dagger,$$
$$A_2(\Omega)^\dagger = -v_{in}(\Omega)^\dagger, \quad A_2(-\Omega)^\dagger = -iA_{in}(-\Omega)^\dagger.$$

In the state picture we have that an arbitrary input state

$$|\psi\rangle = (\mu A_{in}(-\Omega)^\dagger + \nu A_{in}(\Omega)^\dagger)|0\rangle_{Ain}|0\rangle_{vin} \tag{4}$$

is transformed to the output state $|\psi'\rangle$ according to

$$\begin{aligned}|\psi'\rangle = U|\psi\rangle &= U(\mu A_{in}(-\Omega)^\dagger + \nu A_{in}(\Omega)^\dagger)|0\rangle_{Ain}|0\rangle_{vin}\\ &= (\mu UA_{in}(-\Omega)^\dagger U^\dagger + \nu UA_{in}(\Omega)^\dagger U^\dagger)|0\rangle_{A1}|0\rangle_{A2}\\ &= (\mu\imath A_2(-\Omega)^\dagger + \nu A_1(\Omega)^\dagger)|0\rangle_{A1}|0\rangle_{A2}\\ &= \imath\mu|0\rangle_{A1}|1\rangle_{-\Omega,A2} + \nu|1\rangle_{+\Omega,A1}|0\rangle_{A2,}\end{aligned} \tag{5}$$

where U is the unitary operator representing the evolution through the element. In going from lines two to three we have used the fact that $UA_{in}(-\Omega)^\dagger U^\dagger$ is time reversed Heisenberg evolution, obtained explicitly by inverting the standard Heisenberg equations such that the input operator is written in terms of the output operators. We have also used $U|0\rangle_{Ain}|0\rangle_{vin}=|0\rangle_{A1}|0\rangle_{A2}$. We see that the action of an asymmetric Mach-Zehnder on the frequency encoding is equivalent to the action of a polarizing beamsplitter in polarization encoding.

The heart of the rf-HWP is an acousto-optic modulator (AOM). An AOM couples two different frequency and spatial modes together via a phonon interaction [17,18]. In our scheme the AOM is used to shift photons between the two frequencies, $-\Omega$ and Ω. The annihilation operators for the forward traveling outputs of the AOM, $A_3(\omega)$ and $A_4(\omega)$ as defined in Fig. 1, are [17]

$$A_3(\omega) = \cos\,\theta A_1(\omega) + i\,\sin\,\theta A_2(\omega-\delta), \tag{6}$$

$$A_4(\omega) = \cos\,\theta A_2(\omega) + i\,\sin\,\theta A_1(\omega+\delta), \tag{7}$$

where δ represents the modulation frequency applied to the AOM and θ is a measure of the diffraction efficiency of the AOM, such that $\cos\,\theta$ represents the undiffracted fraction of the field and $\sin\,\theta$ represents the diffracted fraction. We have taken the asymmetric phase convention for the AOM outputs and note that θ is proportional to the amplitude of the radio frequency modulation applied to the AOM [18]. We note that the second term in Eq. (6) represents the diffracted, and hence frequency upshifted, component of the input field A_2. Similarly, the second term in Eq. (7)

represents the downshifted component of A_1.

We double pass the AOM in this scheme. The two backward traveling fields A_5 and A_6 emerge from the AOM as illustrated in Fig. 1. The annihilation operators for the backward traveling fields emerging from the AOM are

$$\begin{aligned} A_5(\omega) &= (\cos\theta)A_4(\omega) + i(\sin\theta)A_3(\omega+\delta) \\ &= (\cos 2\theta)A_2(\omega) + i(\sin 2\theta)A_1(\omega+\delta), \end{aligned} \tag{8}$$

$$\begin{aligned} A_6(\omega) &= (\cos\theta)A_3(\omega) + i(\sin\theta)A_4(\omega-\delta) \\ &= (\cos 2\theta)A_1(\omega) + i(\sin 2\theta)A_2(\omega-\delta). \end{aligned} \tag{9}$$

The backward traveling fields A_5 and A_6 make a second pass of the Mach-Zehnder interferometer. The annihilation operators for the output fields of the system, A_{out} and A_{back}, are

$$A_{out}(\omega) = \tfrac{1}{2}[iA_5(\omega)(e^{i\phi}e^{i\omega\tau}+1) + A_6(\omega)(e^{i\phi}e^{i\omega\tau}-1)], \tag{10}$$

$$A_{back}(\omega) = \tfrac{1}{2}[A_5(\omega)(-e^{i\phi}e^{i\omega\tau}+1) + iA_6(\omega)(e^{i\phi}e^{i\omega\tau}+1)], \tag{11}$$

where the parameters ϕ and τ are the same as those for the forward traveling asymmetric Mach-Zehnder interferometer.

We can combine the results of Eqs. (3) and (8)–(11), as well as making use of $A^\dagger(\omega)=A(-\omega)^\dagger$, to arrive at the creation operators for the outputs of the rf-HWP in terms of the inputs. Focusing on the downward traveling output A_{out} at the frequencies of interest $\omega=\pm\Omega$, setting the AOM modulation frequency $\delta=2\Omega$, and setting τ such that $\phi=\pi/2$ and $\Omega\tau=\pi/2$, we find that

$$\begin{aligned} A_{out}(-\Omega)^\dagger &= -[(\cos 2\theta)A_{in}(-\Omega)^\dagger + (\sin 2\theta)A_{in}(\Omega)^\dagger], \\ A_{out}(\Omega)^\dagger &= -[(\cos 2\theta)A_{in}(\Omega)^\dagger - (\sin 2\theta)A_{in}(-\Omega)^\dagger]. \end{aligned} \tag{12}$$

Applying Eq. (12) to the $|0\rangle_L$ input state leads to

$$\begin{aligned} |\psi\rangle_{0,out} &= -[(\cos 2\theta)A_{out}(-\Omega)^\dagger - (\sin 2\theta)A_{out}(\Omega)^\dagger] \\ &\quad\times|0\rangle_{Aout}|0\rangle_{vout} = -[(\cos 2\theta)|0\rangle_L - (\sin 2\theta)|1\rangle_L], \end{aligned} \tag{13}$$

while applying it to the $|1\rangle_L$ input gives

$$\begin{aligned} |\psi\rangle_{1,out} &= -[(\cos 2\theta)A_{out}(\Omega)^\dagger + (\sin 2\theta)A_{out}(-\Omega)^\dagger] \\ &\quad\times|0\rangle_{Aout}|0\rangle_{vout} = -[(\cos 2\theta)|1\rangle_L + (\sin 2\theta)|0\rangle_L]. \end{aligned} \tag{14}$$

Equations (13) and (14) are the key results of this paper. Up to a global phase, these equations are formally equivalent to those used to describe the rotation of an arbitrary two-dimensional vector through the angle $\Theta=2\theta$. Hence, the system illustrated in Fig. 1 is operationally equivalent[1] to a half-wave plate on the basis defined by the frequencies $-\Omega$ and Ω.

III. IN PRACTICE

The situation considered so far is of course impractical, as single frequency qubits will be stationary in time. More realistically, we might consider finite bandwidth qubits of the form

$$\begin{aligned} |0\rangle_L &= \left(\frac{2}{\pi\sigma}\right)^{1/4}\int d\omega e^{-(\Omega+\omega)^2/\sigma}A_{in}(\omega)^\dagger|0\rangle, \\ |1\rangle_L &= \left(\frac{2}{\pi\sigma}\right)^{1/4}\int d\omega e^{-(\Omega-\omega)^2/\sigma}A_{in}(\omega)^\dagger|0\rangle. \end{aligned} \tag{15}$$

The overlap between these qubits is

$$\langle 0|1\rangle_L = e^{-2\Omega^2/\sigma,} \tag{16}$$

Thus, provided the width of the frequency packet is sufficiently small compared to its mean (i.e., $\sigma \ll 2\Omega^2$), then these qubits will be approximately orthogonal. The problem with the finite frequency spread for our device is that now the condition $\Omega\tau=\pi/2$ will not be precisely satified for the entire frequency packet. The effect is to produce a phase shift across the frequency wave packet and also to produce some probability of photons exiting the device in the wrong beam (i.e., A_{back}) or at frequencies outside the computational basis (e.g., 2Ω). Taking such events as lost photons and tracing over them leads to a mixed state, which can be written as

$$\rho_{out,i} = |Q\rangle_i\langle Q|_i + |\overline{Q}\rangle\langle\overline{Q}|, \tag{17}$$

where $\rho_{out,i}$ represents the mixed state output obtained for the logical state input $|i\rangle_L$. For the $|0\rangle_L$ input state

$$\begin{aligned} |Q\rangle_0 = -\left(\frac{2}{\pi\sigma}\right)^{1/4}\int d\omega e^{-(\Omega+\omega)^2/\sigma}[&(\cos 2\theta)A_{in}(\omega)^\dagger \\ &\times 1/2(1+e^{i\pi(\Omega+\omega)/\Omega}) - (\sin 2\theta)A_{in}(\omega+2\Omega)^\dagger \\ &\times 1/4(1+e^{i\pi/2(\Omega+\omega)/\Omega})^2]|0\rangle, \end{aligned} \tag{18}$$

and for the $|1\rangle_L$ input

$$\begin{aligned} |Q\rangle_1 = -\left(\frac{2}{\pi\sigma}\right)^{1/4}\int d\omega e^{-(\Omega-\omega)^2/\sigma}[&(\cos 2\theta)A_{in}(\omega)^\dagger \\ &\times 1/2(1+e^{-i\pi(\Omega-\omega)/\Omega}) + (\sin 2\theta)A_{in}(\omega-2\Omega)^\dagger \\ &\times 1/4(1+e^{-i\pi/2(\Omega-\omega)/\Omega})^2]|0\rangle, \end{aligned} \tag{19}$$

and where $|\overline{Q}\rangle$ is a collective ket representing all the photons that end up in (orthogonal) states outside the computational basis. We can evaluate the impact of this effect by calculat-

[1] A waveplate reflects the polarization of an incoming beam about the optic axis rather than performing an arbitrary rotation through an angle. Hence, technically, the device proposed here is more akin to a Babinet compensator than a waveplate.

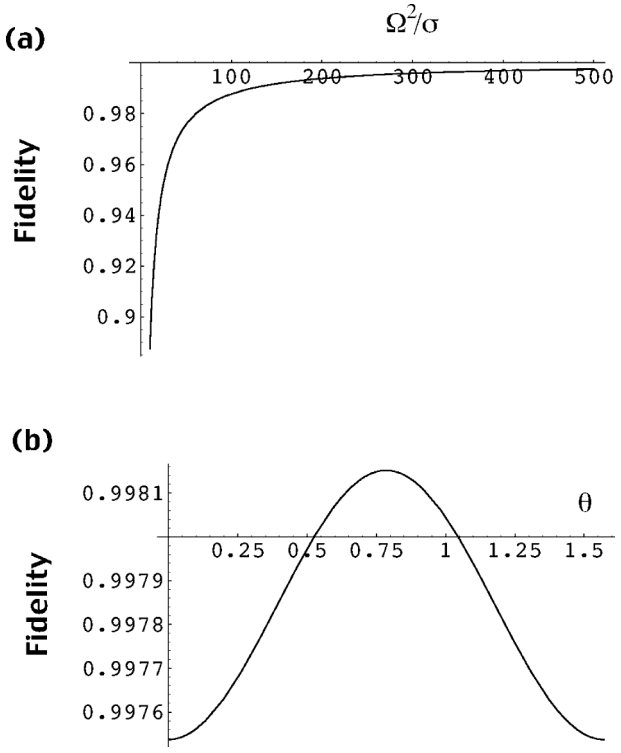

FIG. 2. Fidelity of output vs expected output (a) as a function of the ratio Ω^2/σ with $\theta=\pi/2$ and (b) as a function of θ with $\Omega^2/\sigma=500$.

ing the fidelity between the expected output state, $|P\rangle_i$, and that obtained

$$F=\langle P|\rho_{out,i}|P\rangle_i. \tag{20}$$

The expression for the fidelity is complicated and of limited utility to reproduce here, however, its pertinent features can be listed succinctly: the fidelity depends strongly on the ratio of Ω^2 to σ; it depends weakly on the rotation angle θ; as expected, it tends to 1 as the ratio Ω^2/σ tends to infinity, as illustrated in Fig. 2. Some representative results are: $\Omega^2/\sigma=20$, $F=0.941$; $\Omega^2/\sigma=200$, $F=0.993\,9$; $\Omega^2/\sigma=2000$, $F=0.999\,38$. We conclude that high fidelities are consistent with sensible signal bandwidths.

Let us now turn to technical issues. Conceptually, the rf-HWP comprises a FBS, followed by an AOM, followed by another FBS. However, implementing the rf-HWP in such a fashion would be a tremendously challenging technical task. It would require actively locking the phase $\phi=\pi/2$ in two different interferometers. In addition, the optical path length between the two interferometers would need to be locked. This is why we have proposed the rf-HWP with the folded design illustrated in Fig. 1. This folded design requires the locking of only one interferometer. Further, a locking signal can be derived from the backward traveling output of the rf-HWP, A_{back}, without disturbing the useful output A_{out}.

The technical limitations of the performance of the rf-HWP will be set by the diffraction efficiency of the AOM, the transmission losses of the AOM, and the mode-matching efficiency in the interferometer. Rotation of the input through an angle of $\Theta=\pi/2$ requires that the AOM have a diffraction efficiency of 50%. This technical requirement can be met with commercially available devices [21]. Transmission losses in the AOM mean that the mode which is redirected into the interferometer, and which is ulitmately measured, is actually a mixture of the original mode and the vacuum. This effect may be treated as a perfectly transmitting AOM with a partially transmitting beamsplitter placed on each output port [19,20]. Mode mismatch in the interferometer will reduce the fringe visibility at the sideband frequencies. We can model this effect by decomposing all fields into projections onto an orthonormal basis set of spatial modes, and then introducing a rotation of one of the internal fields of the interferometer relative to the other in this vector space. We treat photons which appear in the incorrect spatial modes as lost.

We can evaluate the impact of AOM losses and mode-matching efficiency by calculating the fidelity between the expected output state and that actually obtained at the output of the rf-HWP. The fidelity after taking account of AOM losses and mode-matching efficiency, F' is

$$F'=F\left(\frac{\eta_{\mathrm{AOM}}}{4}[2(1+\eta_{mm})\cos^2(2\theta)+(1+\sqrt{\eta_{mm}})^2\sin^2(2\theta)]\right)^2, \tag{21}$$

where the single-pass power transmission in the AOM is given by η_{AOM} and the single-pass mode-matching efficiency of the interferometer is given by η_{mm}. The fidelity of the system in the absence of technical limitations is given by F. A good quality free-space AOM would have $\eta>0.95$ [21]. Similarly, a well mode-matched interferometer would have $\eta_{mm}>0.95$ [22]. We note in passing that detector efficiency or homodyne mode-matching efficiency may be modeled in the same way as losses in the AOM.

IV. CONCLUSION

We have proposed devices which may be used as the principle experimental components in optical quantum information systems which make use of the radio frequency basis. These components are essentially the rf-basis analogues of the PBS and the HWP. We have shown that an asymmetric Mach-Zehnder interferometer can perform the function of a FBS. We have also shown that this system may be combined with an acousto-optic modulator in a folded design to form a rf-HWP. We have shown that both devices are feasible using current technologies, and could operate with reasonable bandwidths.

ACKNOWLEDGMENTS

We wish to acknowledge many fruitful discussions with G. N. Milford. This work was supported by the Australian Research Council.

[1] W. T. Buttler *et al.*, Phys. Rev. A **57**, 2379 (1998).
[2] K. Mattle, H. Weinfurter, P. G. Kwiat, and A. Zeilinger, Phys. Rev. Lett. **76**, 4656 (1996).
[3] D. Bouwmeester, J. W. Pan, K. Mattle, M. Eibl, H. Weinfurter, and A. Zeilinger, Nature (London) **390**, 575 (1997).
[4] T. B. Pittman, B. C. Jacobs, and J. D. Franson, Phys. Rev. Lett. **88**, 257902 (2002); T. B. Pittman, M. J. Fitch, B. C. Jacobs, and J. D. Franson, Phys. Rev. A **68**, 032316 (2003).
[5] J. L. O'Brien, G. J. Pryde, A. G. White, T. C. Ralph, and D. Branning, Nature (London) **426**, 6964 (2003).
[6] E. Knill, R. Laflamme, and G. J. Milburn, Nature (London) **404**, 48 (2001).
[7] H. Zbinden, H. Bechmann-Pasquinucci, N. Gisin, and G. Ribordy, Appl. Phys. B: Lasers Opt. **67**, 743 (1998).
[8] E. Lombardi, F. Sciarrino, S. Popescu, and F. De Martini, Phys. Rev. Lett. **88**, 070402 (2002)
[9] M. Fiorentino, P. L. Voss, J. E. Sharping, and P. Kumar, IEEE Photonics Technol. Lett. **14**, 983 (2002).
[10] J. E. Sharping, M. Fiorentino, and P. Kumar, Opt. Lett. **26**, 367 (2001)
[11] C. Silberhorn, P. K. Lam, O. Weiss, F. Konig, N. Korolkova, and G. Leuchs, Phys. Rev. Lett. **86**, 4267 (2001).
[12] J.-M. Merolla, L. Duraffourg, J.-P. Goedgebuer, A. Soujaeff, F. Patois, and W. T. Rhodes, Eur. Phys. J. D **18**, 141 (2002).
[13] E. H. Huntington and T. C. Ralph, J. Opt. B: Quantum Semiclassical Opt. **4**, 123 (2002).
[14] J. Zhang Phys. Rev. A **67**, 054302 (2003)
[15] D. F. Walls and G. J. Milburn, *Quantum Optics* (Springer, Berlin, 1995).
[16] R. J. Glauber, Phys. Rev. **130**, 2529 (1963).
[17] K. J. Resch, S. H. Myrskog, J. S. Lundeen, and A. M. Steinberg, Phys. Rev. A **64**, 056101 (2001).
[18] E. H. Young and S.-K. Yao, Proc. IEEE **69**, 54 (1981).
[19] F. Grosshans and P. Grangier, Eur. Phys. J. D **14**, 119 (2001).
[20] A. I. Lvovsky, H. Hansen, T. Aichele, O. Benson, J. Mlynek, and S. Schiller, Phys. Rev. Lett. **87**, 050402 (2001).
[21] See, for example, http://www.brimrose.com
[22] B. C. Buchler, P. K. Lam, H.-A. Bachor, U. L. Andersen, and T. C. Ralph, Phys. Rev. A **65**, 011803 (2002).